Pergamon

Available online at www.sciencedirect.com

SCIENCE DIRECT®

Cement and Concrete Research 33 (2003) 1399–1405

CEMENT AND CONCRETE RESEARCH

Activation of the fly ash pozzolanic reaction by hydrothermal conditions

S. Goñi, A. Guerrero*, M.P. Luxán, A. Macías

Institute of Construction Science "Eduardo Torroja" CSIC, Serrano Galvache s/n, 28033 Madrid, Spain

Received 6 December 2001; accepted 24 February 2003

Abstract

The effect of hydrothermal treatment on the pozzolanic reaction of two kinds of Spanish fly ashes from coal combustion (ASTM class F) is discussed. Characterization of the compounds formed as a result of hydrothermal treatment and the changes provoked in the starting fly ashes were studied by X-ray diffraction (XRD), scanning electron microscopy (SEM) and infrared (IR) spectroscopy. α-C_2SH, CSH gel, different solid solutions of katoites (the cubic crystallographic variety of hydrogarnets series (C_3ASH_4)) and a mixed oxide ($CaFe_2O_4$) were formed depending on the kind of fly ash. The hydrated compounds are precursors of a new kind of low-energy cement called fly ash belite cement (FABC); besides, they have potential properties to intercalate toxic ions and therefore can be used as immobilization systems of these ions.

Keywords: Hydrothermal; Hydration products; Fly ash; Cement manufacture

1. Introduction

The hydrothermal process is a very useful way to activate reactions whose mechanisms are via dissolution, as is the case of the fly ash pozzolanic reaction. During this process, the acid components of the fly ash are first dissolved, reacting with the basic Ca^{2+} and OH^- ions from the CaO solution. As a result, tobermorite and CSH gel, among others, can be obtained [1–4]. These compounds have potential properties to intercalate ions, such as cesium or strontium [2]; therefore, they can be used for immobilizing toxic wastes. In addition, they can be the precursors of a new kind of low-energy cements called fly ash belite cements (FABC) [4].

Despite the great production of fly ash in Spain, only 20% is employed as a valuable resource, so that storage has become a serious environmental pollution problem. Consequently, the Spanish government is supporting investigation projects to find new applications of those by-products [5–9].

The present paper is part of an extensive investigation in which different kinds of fly ashes (ASTM class F) are hydrothermally treated in the presence of CaO and water. In previous works [10–13], the microstructural evolution and influence of heating temperature on the hydration reaction of the different low-energy FABC were presented. The FABC is considered as a valuable alternative to traditional belite cements, due to the environmental advantage of using fly ash as a raw material, for the low energy consumed in the synthesis process and nonexisting emission of CO_2 to the environment. It was possible to synthesize a hydraulic FABC at a temperature of 700 °C with a dramatic energy reduction in comparison with that necessary in a conventional process (1350 °C).

In this work, characterization of the products formed during hydrothermal treatment of two kind of Spanish fly ashes (ASTM class F, of varying particle size distribution and alkali content), CaO and water is presented. X-ray diffraction (XRD), infrared (IR) spectroscopy and scanning electron microscopy (SEM) analyses were carried out to study the fly ash pozzolanic reaction. The solution was also analyzed and the results were compared with those obtained at room temperature.

2. Experimental

Two kind of Spanish fly ashes called fly ash A (FAA) and B (FAB) were mixed with commercial CaO (analytical

---

* Corresponding author. Tel.: +34-91-302-0400; fax: +34-91-302-0700.

E-mail address: aguerrero@ietcc.csic.es (A. Guerrero).

0008-8846/03/$ – see front matter © 2003 Elsevier Ltd. All rights reserved.
doi:10.1016/S0008-8846(03)00085-1

Table 1
Chemical composition of the two starting fly ashes (percent by weight)

Percentage	FAA	FAB
LOI	5.6	8
IR	0.3	0.2
CaO (total)	4.6	6.7
SiO_2	48.9	45.2
Fe_2O_3	7.4	9.1
Al_2O_3	26.9	25.3
MgO	1.9	1.7
SO_3	0	0
Na_2O	0.67	0.48
K_2O	3.6	3.2
SiO_2 (reactive)	35.8	35.3

LOI = loss on ignition, IR = insoluble residue.

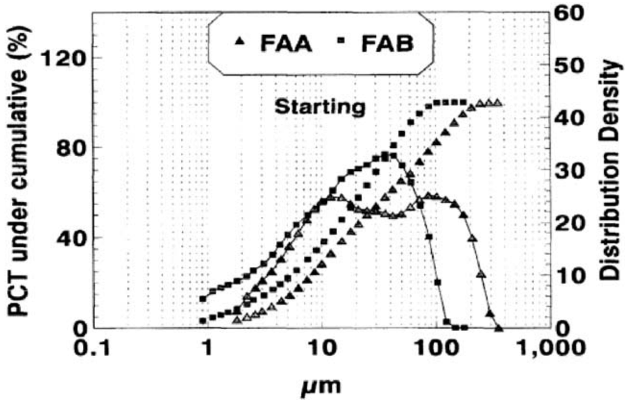

Fig. 2. Particle size distribution curves of starting fly ashes.

reagent grade), at a Ca/Si molar ratio of 2, and demineralized water, at a water to solid ratio of 5. The mixtures were hydrothermally treated at 200 °C, 1.24 MPa during 4 h [13], according to a previous study of Jiang and Roy [4].

The hydrothermal treatment was carried out with a Parr pressure reactor model 4522 (100 ml pump with continuous stirring, split-ring closure and a 4842 temperature controller). XRD patterns were recorded on a Philips PW 1730 diffractometer, graphite monochromator, Cu $K\alpha_1$ radiation. IR study was carried out on a Perkin-Elmer 783 instrument and KBr pellets containing 0.5% of sample. The particle size analyses were made with Sympatec Elos equipment. SEM used a JEOL 5400 microscope with an Oxford EDS microanalysis ISIS model. Samples were coated with gold by sputtering.

3. Results and discussion

3.1. Characterization of starting fly ashes

Table 1 presents the chemical composition of the two fly ashes, which were determined according to the Spanish standard UNE 80215. The alkali content of FAA is higher than that of FAB.

The main crystalline phases detected from XRD (Fig. 1) are SiO_2 (α-quartz), mullite ($Al_6Si_2O_{13}$), CaO and Fe_3O_4. The curves of particle size distribution (Fig. 2) show differences between the two fly ashes. For FAB, the particles are more homogeneous, the majority having diameter ≈ 40 μm. FAA shows two maxima at ≈ 100 and ≈ 12 μm. Both fly ashes meet the requirements for class F of the ASTM specifications and European and Spanish standards (EN-UNE 450).

SEM images of FAA (Fig. 3a and b) and FAB (Fig. 3c) accord with results of particle size distribution (Fig. 2). FAA shows spherical particles of different sizes (cenospheres) with some hollow spheres containing smaller spheres (plerospheres) (Fig. 3a and b); a big and irregular particle of coal can be seen in Fig. 3b. The microstructure of FAB is more homogeneous; all spheres have the same size (diameter ≈ 40 μm). In Table 2, the X-ray microanalysis for the main elements is given for both FAA and FAB as a function of sphere diameter.

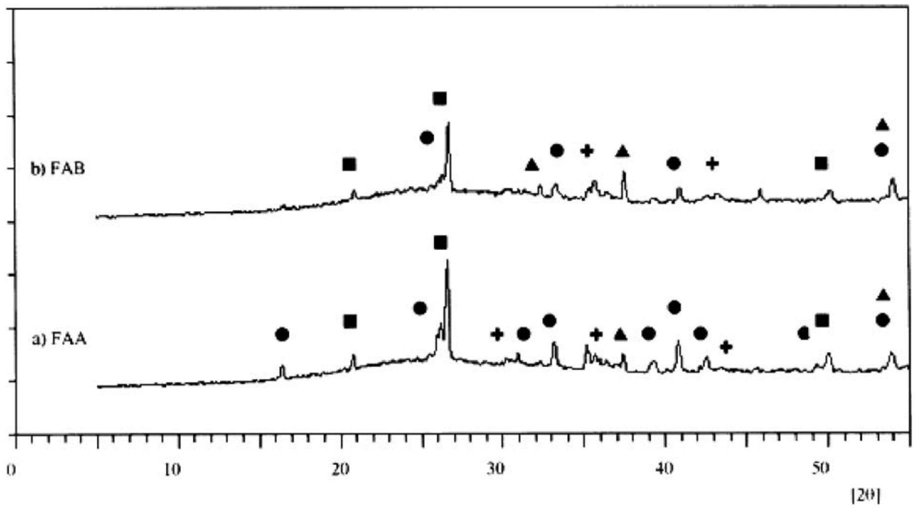

Fig. 1. XRD patterns of the starting fly ashes: ▲ CaO, ● $Al_6Si_2O_{13}$ (A_3S_2), ■ SiO_2, ✚ Fe_3O_4.

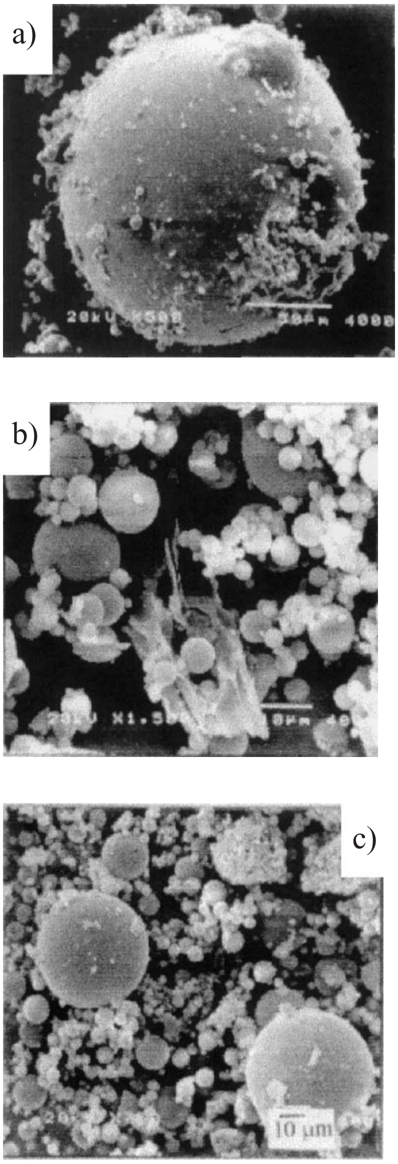

Fig. 3. SEM images of starting fly ashes: (a) FAA; (b) FAA; (c) FAB.

The Fe content increases and the Si content decreases when the sphere diameter decreases. The Al content does not change significantly; as a result, the Al/Fe ratio decreases, and the Al/Si ratio increases slightly with decreasing sphere diameter.

Table 2
X-ray microanalysis of the different diameters of FAA and FAB spheres (percent atom)

	Diameter (μm)	Al	Si	Fe	Al/Si	Al/Fe
FAA	45	0.50	0.73	0.15	0.68	3.3
	10	0.60	0.66	0.17	0.91	3.5
	3	0.44	0.62	0.26	0.71	1.7
	1	0.46	0.48	0.33	0.96	1.4
	Average	0.5	0.6	0.2	0.8	2
FAB	50	0.59	0.70	0.17	0.84	3.5
	25	0.60	0.66	0.18	0.91	3.3
	10	0.47	0.57	0.31	0.82	1.4
	5	0.47	0.50	0.40	0.94	1.2
	Average	0.5	0.6	0.3	0.9	2

3.2. Characterization of fly ash after hydrothermal treatment

3.2.1. SEM and particle size distribution analyses

SEM images of FAA (Fig. 4a and b) after hydrothermal treatment showed that the sphere surfaces appear rough (Fig. 4a) and some are broken (Fig. 4b) (compare with Fig. 3a and b).

In the case of FAB (Fig. 5a–c), the plerospheres (Fig. 3c) are broken and filled with smaller spheres; in general, their surfaces appeared less attacked than those of FAA (Fig. 4a and b).

X-ray microanalysis (Table 3) revealed that in both FAA and FAB the Al/Si ratio tends to increase as the sphere diameter decreases. The Al/Fe ratio increases in the smallest spheres for FAA and decreases strongly for the FAB. The average Al/Si ratio is low for FAB after hydrothermal treatment.

The particle size distribution for FAA (Fig. 6) shows an increase of the maximum centred at ≈10–20 μm with respect to the one centred at ≈100–120 μm, which indicates a shift to a lower particle size in comparison with the results of Fig. 2. Similarly, for FAB, the peak centred at ≈10–20 μm is higher than that centred at ≈30–40 μm.

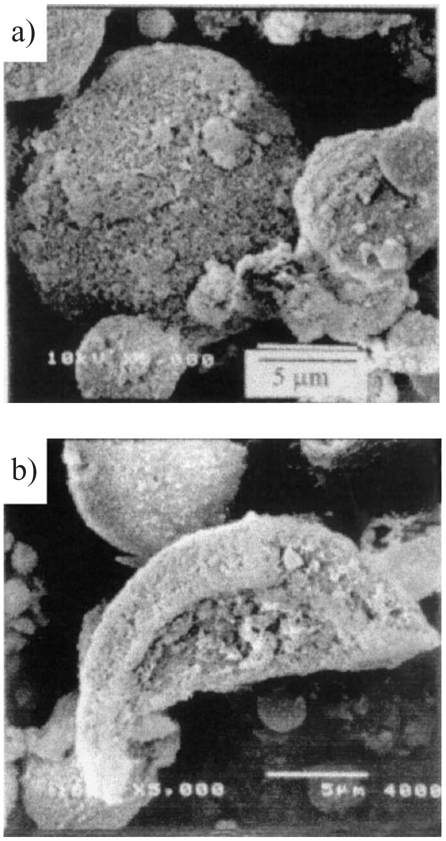

Fig. 4. SEM images of FAA after hydrothermal treatment.

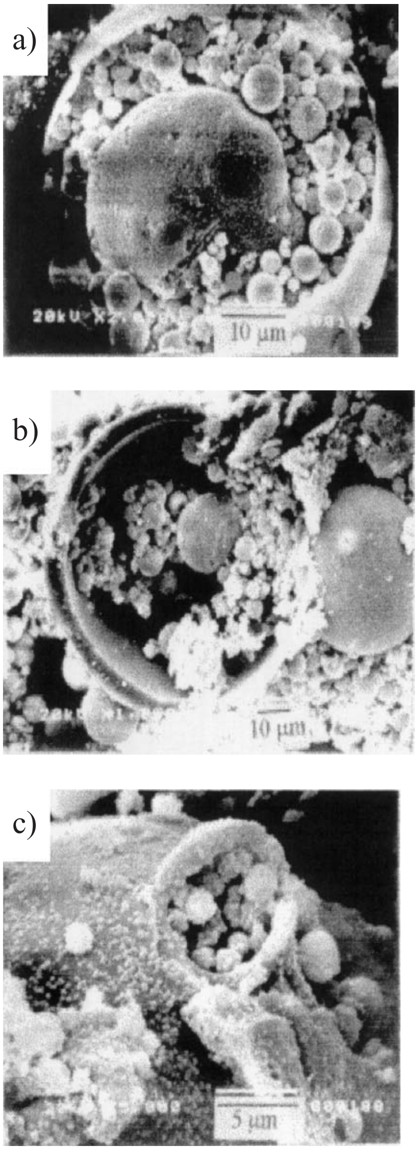

Fig. 5. SEM images of FAB after hydrothermal treatment.

These behaviours could be related to rupture of the big plerospheres and consequently an increase in amount of the small cenospheres especially for FAB.

Table 3
X-ray microanalysis of the different diameters of FAA and FAB spheres after hydrothermal treatment (percent atom)

	Diameter (μm)	Al	Si	Fe	Al/Si	Al/Fe
FAA	100	0.38	0.61	0.35	0.62	1.1
	15	0.45	0.59	0.33	0.76	1.4
	5	0.71	0.55	0.15	1.3	4.7
	1	0.51	0.59	0.26	0.86	2
	Average	0.5	0.6	0.3	0.9	2
FAB	50	0.57	1.02	0.04	0.56	14
	20	0.39	1.08	0.08	0.36	5.2
	8	0.24	0.38	0.41	0.63	0.58
	1	0.64	0.78	0.74	0.82	0.86
	Average	0.5	0.8	–	0.6	–

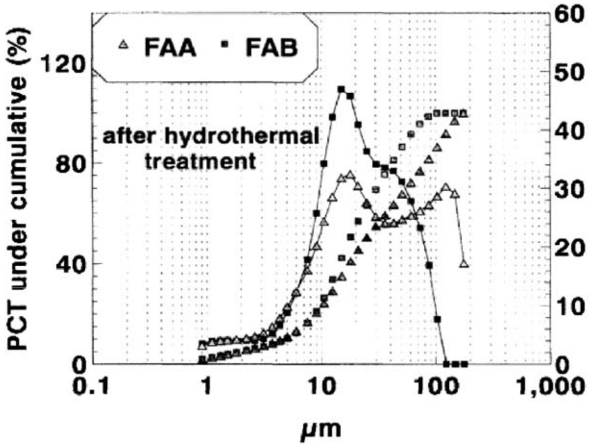

Fig. 6. Particle size distribution curves of fly ashes after the hydrothermal treatment.

3.2.2. XRD analyses

The main crystalline compounds detected by XRD after hydrothermal treatment of fly ash, CaO and water (Fig. 7) are α-C_2SH, different solid solutions of katoites (C_3ASH_4), calcite ($CaCO_3$), portlandite ($Ca(OH)_2$) and traces of tobermorite ($Ca_5Si_6H_2O_{18}\cdot 4H_2O$) and $CaFe_2O_4$.

In the case of FAB (Fig. 7b), all reflections appear shifted with respect to the reflections of FAA (Fig. 7a); this shift could be indicated by the presence of new phases, which do not have a well crystallinity. In both cases, a shoulder appears in all the C_3ASH_4 (katoite) reflections at lower 2θ values, which could suggest solid solution of Fe-katoite ($C_3A_{0.5}F_{0.5}SH_4$) in the case of FAA and the carbonated katoite ($C_3AS_3c_3H_{1.5}$) being the iron combined as a mixed oxide: $CaFe_2O_4$ in FAB. It was not possible to discover the presence of CSH gel by XRD due to overlapping calcite reflections and because CSH converts to tobermorite (Ca_5Si_6 $H_2O_{18}\cdot 4H_2O$), the conversion time depends on alkali concentration [2]. The SiO_2 (α-quartz) and mullite reflections disappear in both samples. The hydrogarnet solid solutions could be related to the Al/Si and Al/Fe ratios of the small fly ash spheres, which are the first to react. The mixed oxide $CaFe_2O_4$ detected in the case of the FAB is consistent with the high Fe content in small spheres.

The crystalline compounds detected by XRD differ from those reported previously. Jiang and Roy [4] obtained CSH gel and C_3AH_6 from a mixture of class F fly ash, lime and water (Ca/Si = 2) after heating, first up to 80 °C in stirred suspensions for 10 h and then heated hydrothermally 4 h at 200 °C under saturated steam pressure.

Ma and Brown [1] studied the hydrothermal behaviour of oxide mixtures, which simulate fly ash, using phase-pure starting materials and class F fly ashes whose compositions were adjusted to those of the pure oxide mixtures. In the first case called Model System I: $Ca/(Si+Al) = 0.37$, $Al/(Si+Al) = 0.24$ and $Na/Si = 0$ and 0.12, the CSH gel was formed as a major product regardless of the treatment temperature (pure oxides mixed with deion-

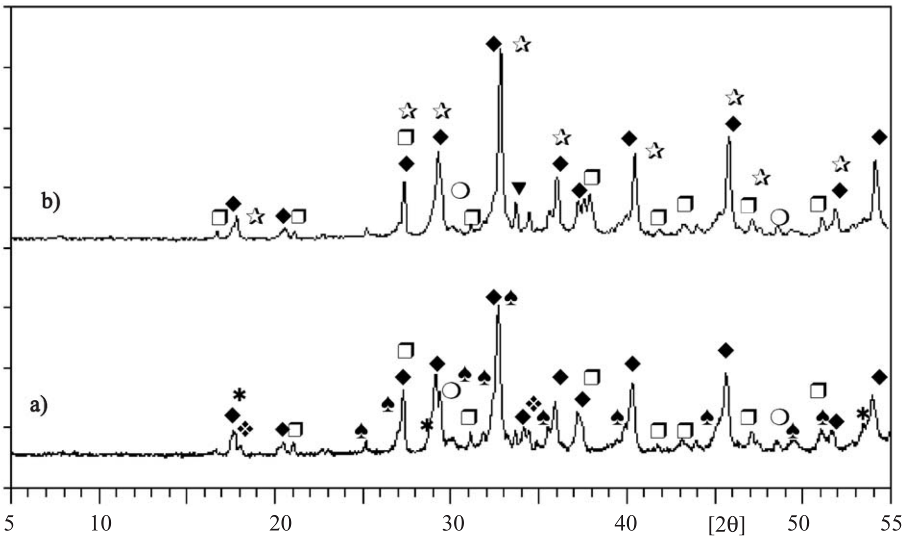

Fig. 7. XRD patterns of reacted fly ashes: (a) reacted FAA and (b) reacted FAB: □ C_2SH ($Ca_2SiO_4{\cdot}H_2O$), ◆ C_3ASH_4 ($Ca_3Al_2(SiO_4)(OH)_8$), ♠ $Ca_5Si_6H_2O_{18}{\cdot}4H_2O$, * $C_3A_{0.5}F_{0.5}SH_4$ ($Ca_3AlFe(SiO_4)(OH)_8$), ☆ $C_3AS_3C_3H_{1.5}$ ($Ca_3Al_2(SiO_4, CO_3, OH)_3$), ▼ CF ($CaFe_2O_4$), ❖ CH ($Ca(OH)_2$), ○ Cc ($CaCO_3$).

ized water were treated for 24 h at 25, 60, 100 and 180 °C). For similar samples treated in 0.1 M NaOH solution, CSH gel was also the dominant phase. The authors concluded that NaOH activation is not required in this temperature range.

In the case of class F fly ash, the composition was adjusted to the Model System II: Ca/(Si + Al) = 0.8, Al/(Si + Al) = 0.15 and Na/Si = 0.05 and 0.3 (suggested for synthesizing tobermorite). After 2 h of hydrothermal treatment at 170 °C in 0.8 M NaOH, CSH gel is formed which converts tobermorite ($Ca_5Si_6H_2O_{18}{\cdot}4H_2O$) and katoite after 12 h of reaction. The authors concluded that NaOH accelerates the kinetics of tobermorite formation.

The main differences reported in the present work are related to the α-C_2SH, the phase hydrothermally synthesized by Heller [19] from the β-C_2S heated for 40 days at 150 °C, and the different solid solution of katoite types, which could be attributed, among other causes, to the different Ca/(Si + Al) and Al/(Si + Al) molar ratios of 1.2 and 0.40, respectively, in comparison with those used by Ma and Brown. In addition, the particle size distribution of the starting fly ashes and the changes provoked by the hydrothermal treatment could influence the products formed because the composition of the smaller spheres also changes, as verified in the present work.

3.2.3. IR spectroscopy analyses

From IR spectroscopy, two main types of compounds can be identified in the samples: silicates and carbonates. As can be seen in Fig. 8, a strong absorption zone between 800 and 1100 cm^{-1} with three maxima at 1000, 960 and 870 cm^{-1} is produced for the reacted FAA (Fig. 8a) and with two maxima at 970 and 870 cm^{-1} for reacted FAB (Fig. 8b). The presence of calcite produces a wide band with two maxima at 1485 and 1420 cm^{-1}; at 870 and 760 cm^{-1}, intensities are lower in the case of reacted FAB (Fig. 8b).

The hydrated calcium silicates formed during the hydrothermal treatment (α-C_2SH and CSH gel) could be identified by the absorptions appeared at 1000 [14] and 960–970 cm^{-1} [15], respectively. The higher intensity of those bands for reacted FAA would indicate a higher pozzolanic reaction degree for this FAA.

The strong and broad band located between 3900 and 3200 cm^{-1} stretching region is due to the lattice water and OH^- group vibration, the latter at 3700 and 3560 cm^{-1} [16]. The bands centred at 870, 680 and 460–470 cm^{-1} could be related to the AlO_2^- groups of the katoite series [17].

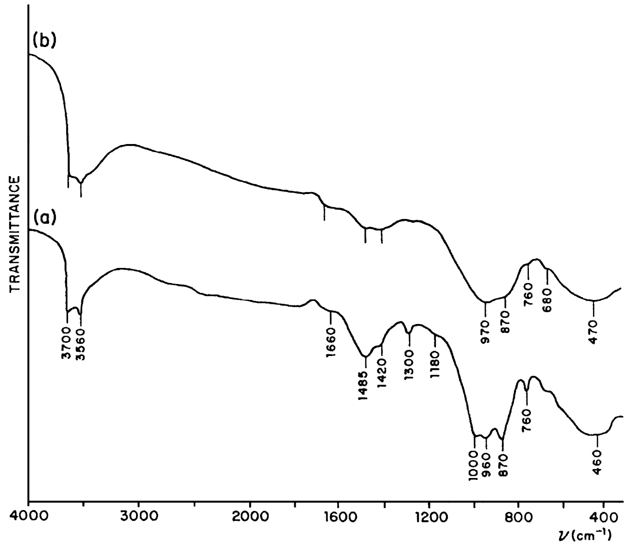

Fig. 8. IR spectra of reacted fly ashes: FAA (a) and FAB (b).

3.2.4. Analyses of the solutions

The pozzolanic reactivity, in the case of samples treated at room temperature, was evaluated according to a previous pozzolanic activity test [18]. This test assesses the pozzolanicity, comparing the quantity of calcium hydroxide in the aqueous solution in contact to the fly ash, after a fixed period of time at 40 ± 1 °C, with the quantity of calcium hydroxide capable of saturate a solution of the same alkalinity. The test is considered positive if the concentration of calcium hydroxide in the solution is lower than the saturation concentration (see continuous curve in Fig. 9). The pozzolanicity was evident after 28 days in both FAA and FAB, being higher in the case of FAA. The Ca^{2+} and OH^- concentrations, in the case of the solutions hydrothermally treated, have not been included in the graph because the saturation concentration with respect to the calcium hydroxide is unknown in the hydrothermal conditions here studied.

The alkali Na^+ and K^+ concentrations, and especially K^+ concentration, dramatically increase compared with those treated at 40 °C (Fig. 10), the values higher for the FAA.

These high alkali concentrations are due to the dissolution of the fly ash particles. As pozzolanic reaction takes place via fly ash dissolution, the alkali concentration could be indicative of reactivity.

The solution analyses evidence that the hydrothermal treatment increased strongly the fly ash pozzolanic reactivity, especially in FAA; however, these results are not consistent with the particle size distribution presented in Fig. 6, where the FAA contains higher amount of big particles.

One of the reasons to explain this contradiction could be related to the alkalis. As shown in Fig. 10, the Na^+ and K^+ of the starting fly ashes are fastly released to the solution, this process being more significant for FAA. This alkali liberation is produced as a consequence of the pozzolanic reaction, which takes place via dissolution; in addition, the alkalinity increases the dissolution of the fly ash acid components, as is the case of Si whose relative content, determined from X-ray microanalysis, is significantly lower for FAA compared with FAB (see Table 3). Consequently, it seems to deduce that on hydrothermal condition the alkalis play a role more important than the fineness of the starting fly ashes in their reactivity.

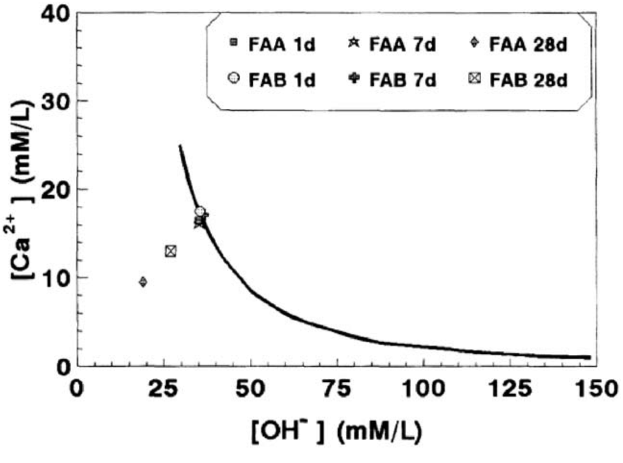

Fig. 9. Results of the fly ash pozzolanic activity test at ambient temperature.

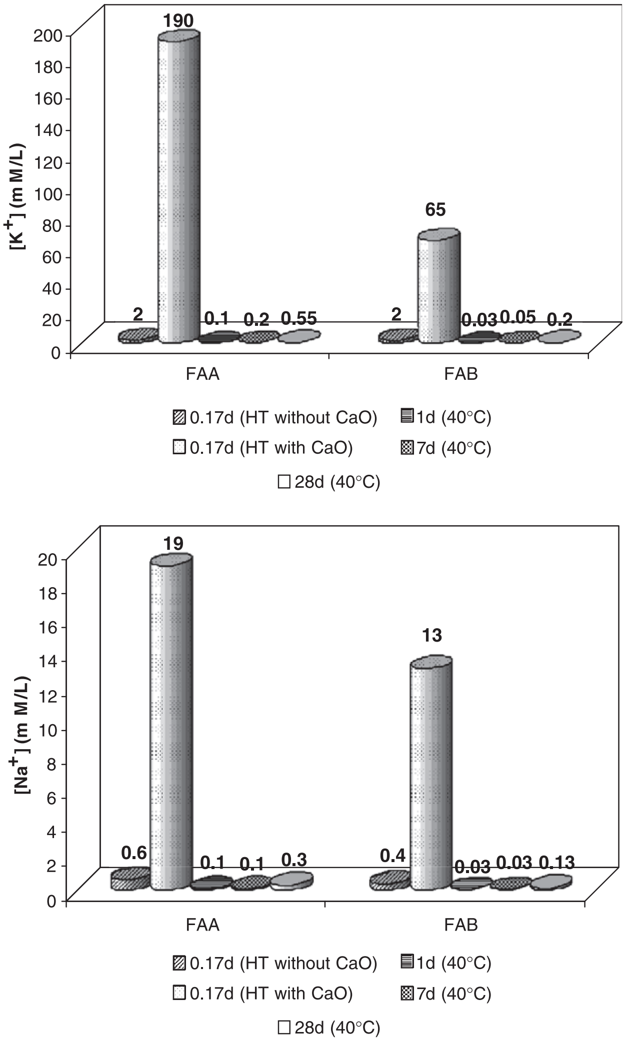

Fig. 10. Alkali (Na^+ and K^+) concentrations of the solutions at the different conditions studied.

Acknowledgements

The authors are thankful for the financial support of the CICYT (project no. MAT 95-0054) and the Power Station of Soto de Ribera and Velilla de Rio Carrion for the fly ash supplied.

References

[1] W. Ma, P.W. Brown, Hydrothermal synthesis of tobermorite from fly ashes, Adv. Cem. Res. 9 (33) (1997) 9–16.

[2] W. Ma, P.W. Brown, Sequestration of cesium and strontium by tober-

morite synthesized from fly ashes, J. Am. Ceram. Soc. 6 (1996) 1707–1710.

[3] W. Ma, P.W. Brown, Hydrothermal reactions of fly ash with $Ca(OH)_2$ and $CaSO_4 \cdot 2H_2O$, Cem. Concr. Res. 27 (8) (1997) 1237–1248.

[4] W. Jiang, D.M. Roy, Hydrothermal processing of new fly ash cement, Ceram. Bull. 71 (4) (1992) 642–647.

[5] P. Lorenzo, S. Goñi, S. Hernández, A. Guerrero, Effect of fly ashes with high total alkali content on the alkalinity of the pore solution of hydrated Portland cement, J. Am. Ceram. Soc. 79 (2) (1996) 470–474.

[6] S. Goñi, M.P. Lorenzo, A. Guerrero, M.S. Hernández, Calcium hydroxide saturation factors in the pore solutions of hydrated Portland cement fly ash pastes, J. Am. Ceram. Soc. 79 (4) (1996) 1041–1046.

[7] M.P. Lorenzo, C. Alonso, S. Goñi, M. Acha, Fly ash application to the reinforced concrete: durability, III Congreso Internacional de Química de la ANQUE, "Solid and Liquid Wastes: Their Best Destination (II)", vol. III, Asociaciòn Nacional de Químicos de España, Puerto de la Cruz, Tenerife, 1994, pp. 119–129.

[8] S. Goñi, M.P. Lorenzo, M.S. Hernández, A. Guerrero, The role of the fly ash aluminous component on the durability of the Portland-fly ash pastes in sulfated medium: Part I. Characterization of the solid phase, 4th CANMET/ACI International Conference on Durability of Concrete, Sydney, American Concrete Institute, USA, 1997, Poster Session.

[9] M.P. Lorenzo, S. Goñi, A. Guerrero, M.S. Hernández, The role of the fly ash aluminous component on the durability of the Portland-fly ash pastes in sulfated medium: Part II. Characterization of the pore solution, 4th CANMET/ACI International Conference on Durability of Concrete, Sydney, American Concrete Institute, USA, 1997, Poster Session.

[10] S. Goñi, M.P. Luxán, A. Guerrero, M.S. Hernández, A. Macías, Microstructural study of hydration reactions of a fly ash-belite cement, in: V.M. Malhotra (Ed.), Proceedings of the Sixth CANMET/ACI International Conference on Fly Ash, Silica Fume, Slag and Natural Pozzolans in Concrete, Bangkok, vol. 1. American Concrete Institute, 1998, pp. 207–224.

[11] S. Goñi, A. Guerrero, A. Macías, M.P. Luxán, Effect of the synthesis temperature on the hydration reaction of fly ash-belite cement, in: M. Cohen, S. Mindess, J. Skalny (Eds.), Materials Science of Concrete: The Sydney Diamond Symposium, American Ceramic Society, 1998, pp. 93–108.

[12] S. Goñi, M.P. Luxán, M.S. Hernández, A. Guerrero, Synthesis and characterization of a belite cement from hydrothermal activation of fly ashes, 4th CANMET/ACI International Conference on Durability of Concrete, Sydney, American Concrete Institute, USA, 1997, Book of Abstract.

[13] S. Goñi, A. Guerrero, M.P. Luxán, A. Macías, Dehydration of pozzolanic products hydrothermally synthesized from fly ashes: microstructure evolution, Mater. Res. Bull. 35 (2000) 1333–1344.

[14] Y. Nanro, Z. Baigian, M. Zhanwen, An active β-dicalcium preparation and hydration, 8th Int. Congr. Chem. Cem., Brazil, vol. III, Rio de Janeiro, Brazil, 1986, pp. 23–27.

[15] T. Mitsuda, S. Kobayakawa, H. Toraya, Characterization of hydrothermally formed CSH, 8th Int. Congr. Chem. Cem., Brazil, vol. III, Rio de Janeiro, Brazil, 1986, pp. 176–178.

[16] K. Nakamoto, Infrared and Raman Spectra of Inorganic and Coordination Compounds, 4th ed., Wiley, 1986.

[17] R.A. Nyquist, R.O. Kagel, Infrared Spectra of Inorganic Compounds, Academic Press, New York, 1971.

[18] M.P. Luxán, T. Vázquez, The silica gel as a standard pozzolana: its hard activity and its limitations, Cemento 3 (1974) 113–130.

[19] L. Heller, Acta Crystallogr. 5 (1952) 724.